Supporting Information

Modeling the effects of interfacial characteristics on gas permeation behavior of nanotube-mixed matrix membranes

Ehsan Chehrazi [1], Alireza Sharif [1], Mohammadreza Omidkhah [2], Mohammad Karimi [3]*

[1] Department of Polymer Reactions Engineering, Faculty of Chemical Engineering, Tarbiat Modares University, P.O. Box: 14155-143, Tehran, Iran

[2] Faculty of Chemical Engineering, Tarbiat Modares University, P.O. Box: 14115-143, Tehran, Iran

[3] Department of Textile Engineering, Amirkabir University of Technology, Hafez Avenue, P.O. Box: 15914, Tehran, Iran

* Corresponding author. E-mail: asharif@modares.ac.ir

S1- The equations used for developing the new model

Nan et al[1] proposed a general formulation for the effective thermal conductivity, K_{eff}, of a polymer-ellipsoidal particle composite considering the interfacial thermal resistance between the polymer and particles according to the multiple scattering theory:[2]

$$K_{eff} = K_m \frac{1+\varphi\left[\beta_{11}(1-L_{11})\left(1-\langle cos^2\theta\rangle\right)+\beta_{22}(1-L_{22})\langle cos^2\theta\rangle\right]}{1-\varphi\left[\beta_{11}L_{11}(1-\langle cos^2\theta\rangle)+\beta_{22}L_{22}\langle cos^2\theta\rangle\right]} \quad \text{(S1)}$$

where

$$\langle cos^2\theta\rangle = \frac{\int \rho(\theta) cos^2\theta \sin\theta \, d\theta}{\int \rho(\theta) \sin\theta \, d\theta} \quad \text{(S2)}$$

$$\beta_{11} = \frac{K_{11} - K_m}{K_m + L_{11}(K_{11} - K_m)} \quad \text{(S3)}$$

$$\beta_{22} = \frac{K_{22} - K_m}{K_m + L_{22}(K_{22} - K_m)} \quad \text{(S4)}$$

where K_m, K_{ii} (i: 1, 2) and L_{ii} (i: 1, 2) are the thermal conductivity of matrix, equivalent thermal conductivities along the X_i symmetric axis of ellipsoidal composite and a geometrical factor, respectively. Also, θ is the angle between the materials axis and the local particle symmetric axis, $\rho(\theta)$ is a distribution function describing the ellipsoidal particle orientation and φ is the volume fraction of particles. Equation S1 considers the effects of size, shape, orientation and volume fraction of fillers as well as the interfacial thermal resistance between the filler and polymer (by the term β_{ii}). The Nan model can be simplified for isotropic composites with completely random oriented ellipsoidal particles ($\langle\cos^2\theta\rangle = 1/3$) as:

$$K_{eff} = K_m \frac{3 + \varphi\left[2\beta_{11}(1 - L_{11}) + \beta_{22}(1 - L_{22})\right]}{3 - \varphi\left[2\beta_{11}L_{11} + \beta_{22}L_{22}\right]} \quad \text{(S5)}$$

Equations S3-S5 can be adopted for uniformly distributed tubular filler-containing polymers by considering $L_{11} = 0.5$ and $L_{22} = 0$ (eqs S6-S8, respectively): [3]

$$\beta_{11} = \frac{2(K_{11} - K_m)}{K_{11} + K_m} \quad \text{(S6)}$$

$$\beta_{22} = K_{22}/K_m - 1 \quad \text{(S7)}$$

$$\frac{K_{eff}}{K_m} = \frac{3 + \varphi(\beta_{11} + \beta_{22})}{3 - \varphi\beta_{11}} \quad \text{(S8)}$$

where φ is the volume fraction of nanotubes. K_{11} and K_{22} are the thermal conductivities along transverse and longitudinal axes of the nanotube coated with a thin interfacial layer, respectively, as schematically shown in Figure S1.

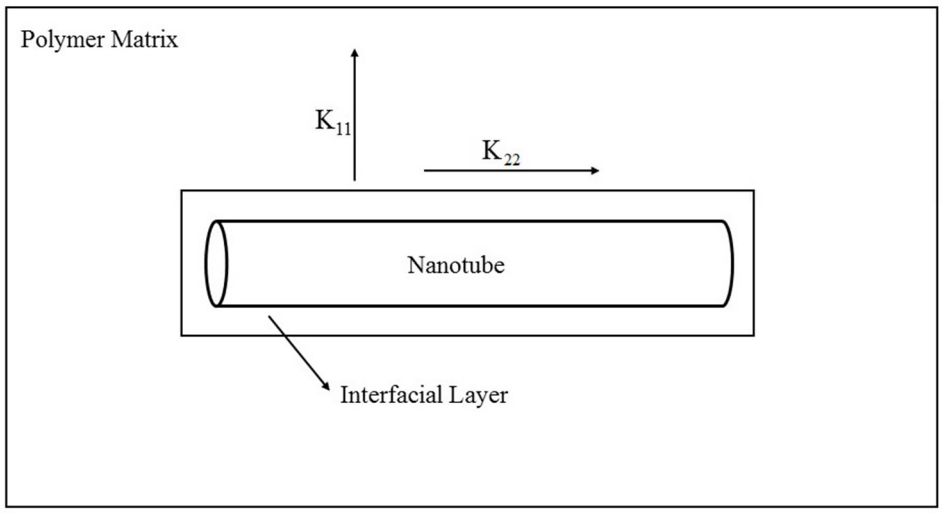

Figure S1. Schematic illustration of thermal conduction through transverse (11) and longitudinal (22) axes of a nanotube embedded in a polymer matrix.

The transverse and longitudinal thermal conductivities of the nanotube particles are calculated from the series resistance of interface/nanotube/interface model as follows:[3]

$$K_{11} = \frac{K_{NT}}{1 + \frac{2a_k}{d}\frac{K_{NT}}{K_m}} \quad \text{(S9)}$$

$$K_{22} = \frac{K_{NT}}{1 + \frac{2a_k}{L}\frac{K_{NT}}{K_m}} \quad \text{(S10)}$$

where K_{NT}, L and d are the thermal conductivity, length and diameter of the nanotube (NT), respectively. Also, a_k is a so-called Kapitza radius and is defined by:[4]

$$a_k = R_k \cdot K_m \qquad \text{(S11)}$$

where R_k is the "interfacial thermal resistance" between the nanotube and polymer matrix. Finally, by substituting eqs S9 and S10 into eqs S6 and S7, respectively, the thermal conductivity of a nanotube composite (eq S8) is obtained as:[1]

$$\frac{K_{eff}}{K_m} = 1 + \frac{\varphi \cdot \alpha}{3} \frac{K_{NT}/K_m}{\alpha + \frac{2a_k}{d}\frac{K_{NT}}{K_m}} \qquad \text{(S12)}$$

where α is the aspect ratio of nanotubes. The Nan model demonstrates that the existence of polymer-nanotube (NT) interfacial thermal resistance decreases the thermal conductivity of the polymer/NT nanocomposite.

S2- Experimental data from the literature used for validating the proposed model

Tables S1-S4 represent the existing experimental data in the literature including 10 sets of CO_2/CH_4 permeation, 12 sets of CO_2/N_2 permeation, 3 sets of CO_2/O_2 permeation and 2 sets of CO_2/H_2 permeation through CNT- or HNT-containing MMMs.

Table S1. Experimental CO_2/CH_4 separation data of different nanotube-MMMs.

Set	MMMs	Φ (vol%)	Permeability (Barrer)	$P(CO_2)/P(CH_4)$
			$P(CO_2)$	
1	MWCNT/PVAm [5]	0.0	19.6	12.1
		5.0	29.9	10.0
2	MWCNT-NH_2/PVAm [5]	0.0	19.6	12.1
		5.0	28.3	15.6
3	MWCNT-PMMA/PA [6]	0.0	8.23	26.6
		2.0	8.71	20.6
4	Milled-MWCNT-PMMA/PA [6]	0.0	8.23	26.6
		2.0	10.6	29.0
5	MWCNT-NH_2/Pebax [7]	0.0	130	17.0
		5.0	195	17.0
		13	286	17.0
		18	390	16.0
6	HNT/PEI [8]	0.0	0.63	79.6
		0.5	1.47	15.1
7	HNT-NH_2/PEI [8]	0.0	0.63	79.6
		0.25	0.80	85.9

		0.50	1.17	47.8
8	HNT-PANi/PSf [9]	0.0	17.4	21.6
		0.25	30.4	23.8
		0.50	46.5	26.6
		1.0	68.4	14.1
9	HNT/PI [10]	0.0	640	23.7
		10	950	20.2
10	HNT-NH_2/PI [10]	0.0	640	23.7
		10	910	22.8

Table S2. Experimental CO_2/N_2 separation data of different nanotube-MMMs.

Set	MMMs	Φ (vol%)	Permeability (Barrer)	$P(CO_2)/P(N_2)$.
			$P(CO_2)$	
1	MWCNT-COOH/PES [11]	0.0	2.70	21.5
		1.0	3.20	22.5
		2.0	3.50	22.0
		4.0	4.50	22.5
2	SWCNT/BPPOdp [12]	0.0	78.0	30.0
		3.0	122	29.0
		6.0	156	29.0
3	SWCNT-COOH/BPPOdp [12]	0.0	78.0	30.0
		3.0	79.0	30.0
4	MWCNT/BPPOdp [12]	0.0	78.0	30.0
		3.0	110	32.0
		6.0	148	31.0
5	MWCNT/PI, in situ polymerization [13]	0.0	2.31	15.4
		0.7	3.32	18.4
		1.4	4.58	20.8

		2.1	5.44	22.7
6	MWCNT-COOH/PI, in situ polymerization [13]	0.0	2.31	15.4
		0.7	4.79	26.6
		1.4	6.77	32.2
		2.1	9.06	37.7
7	MWCNT-COOH/PI, solution mixing [13]	0.0	2.31	15.4
		0.7	3.67	20.4
		1.4	5.15	26.2
		2.1	6.12	29.1
8	MWCNT/PVAm [5]	0.0	19.6	25.2
		5.0	29.9	15.7
9	MWCNT-NH_2/PVAm [5]	0.0	19.6	25.2
		5.0	28.3	21.3
10	HNT-PANi/PSf [9]	0.0	17.4	25.4
		0.25	30.4	26.1
		0.5	46.5	27.3
		1.0	68.4	22.1
11	HNT/PI [10]	0.0	640	25.6
		10	950	17.6
12	HNT-NH_2/PI [10]	0.0	640	29.6
		10	910	20.2

Table S3. Experimental CO_2/O_2 separation data of different nanotube-MMMs.

Set	MMMs	Φ (vol%)	Permeability (Barrer)	$P(CO_2)/P(O_2)$
			$P(CO_2)$	
1	MWCNT/PVAm [5]	0.0	19.6	9.98
		5.0	29.9	8.91
2	MWCNT-NH_2/ PVAm [5]	0.0	19.6	9.98
		5.0	28.3	10.8
3	HNT-PANi-PSf [9]	0.0	17.4	4.37
		0.25	30.4	4.35
		0.5	46.5	4.63
		1.0	68.4	3.63

Table S4. Experimental CO_2/H_2 separation data of different nanotube-MMMs.

Set	MMMs	Φ (vol%)	Permeability (Barrer)	
			$P(CO_2)$	$P(CO_2)/P(H_2)$
1	MWCNT/PVA [14]	0.0	850	77.9
		1.0	856	44.9
		2.0	917	41.0
		4.0	921	40.5
2	MWCNT-NH_2/PVA [15]	0.0	986	54.0
		3.0	1014	54.0

S3- An example describing the calculation of the parameter %AARE

For example, the parameter *%AARE* for set 5 of Table 3 is obtained according to eq 21 as follows:

HC model:

$$\%AARE = \frac{100}{4}\left(\left|\frac{2{\cdot}31-2{\cdot}31}{2{\cdot}31}\right| + \left|\frac{2{\cdot}40-3{\cdot}32}{3{\cdot}32}\right| + \left|\frac{2{\cdot}50-4{\cdot}58}{4{\cdot}58}\right| + \left|\frac{2{\cdot}59-5{\cdot}44}{5{\cdot}44}\right|\right) = 31 \cdot 32$$

KJN model:

$$\%AARE = \frac{100}{4}\left(\left|\frac{2{\cdot}31-2{\cdot}31}{2{\cdot}31}\right| + \left|\frac{2{\cdot}33-3{\cdot}32}{3{\cdot}32}\right| + \left|\frac{2{\cdot}34-4{\cdot}58}{4{\cdot}58}\right| + \left|\frac{2{\cdot}36-5{\cdot}44}{5{\cdot}44}\right|\right) = 33 \cdot 86$$

Proposed model:

$$\%AARE = \frac{100}{4}\left(\left|\frac{2{\cdot}31-2{\cdot}31}{2{\cdot}31}\right| + \left|\frac{3{\cdot}38-3{\cdot}32}{3{\cdot}32}\right| + \left|\frac{4{\cdot}45-4{\cdot}58}{4{\cdot}58}\right| + \left|\frac{5{\cdot}51-5{\cdot}44}{5{\cdot}44}\right|\right) = 1 \cdot 50$$

References

(1) Nan, C.-W.; Birringer, R.; Clarke, D. R.; Gleiter, H. Effective Thermal Conductivity of Particulate Composites with Interfacial Thermal Resistance. *J. Appl. Phys.* **1997,** *81*, 6692-6699.
(2) Gubernatis, J. E.; Krumhansl, J. A. Macroscopic Engineering Properties of Polycrystalline Materials: Elastic Properties. *J. Appl. Phys.* **1975,** *46* (5), 1875-1883.
(3) Nan, C.-W.; Liu, G.; Lin, Y.; Li, M. Interface Effect on Thermal Conductivity of Carbon Nanotube Composites. *Appl. Phys. Lett.* **2004,** *85*, 3549-3551.
(4) Tonpheng, B.; Yu, J.; Andersson, O. Thermal conductivity, heat capacity, and cross-linking of polyisoprene/single-wall carbon nanotube composites under high pressure. *Macromolecules* **2009,** *42* (23), 9295-9301.

(5) Wang, M.; Wang, Z.; Li, N.; Liao, J.; Zhao, S.; Wang, J.; Wang, S. Relationship Between Polymer–Filler Interfaces in Separation Layers and Gas Transport Properties of Mixed Matrix Composite Membranes. *J. Membr. Sci.* **2015,** *495*, 252-268.
(6) Wong, K.; Goh, P.; Ismail, A. Gas Separation Performance of Thin Film Nanocomposite Membranes Incorporated with Polymethyl Methacrylate Grafted Multi-Walled Carbon Nanotubes. *Int. Biodeterior. Biodegrad.* **2015,** *102*, 339-345.
(7) Zhao, D.; Ren, J.; Li, H.; Li, X.; Deng, M. Gas Separation Properties of Poly (amide-6-b-ethylene oxide)/amino Modified Multi-Walled Carbon Nanotubes Mixed Matrix Membranes. *J. Membr. Sci.* **2014,** *467*, 41-47.
(8) Hashemifard, S. A.; Ismail, A. F.; Matsuura, T. Mixed Matrix Membrane Incorporated with Large Pore Size Halloysite Nanotubes (HNT) as Filler for Gas Separation: Experimental. *J. Colloid Interface Sci.* **2011,** *359* (2), 359-370.
(9) Murali, R. S.; Padaki, M.; Matsuura, T.; Abdullah, M.; Ismail, A. F. Polyaniline in Situ Modified Halloysite Nanotubes Incorporated Asymmetric Mixed Matrix Membrane for Gas Separation. *Sep. Purif. Technol.* **2014,** *132*, 187-194.
(10) Ge, L.; Lin, R.; Wang, L.; Rufford, T. E.; Villacorta, B.; Liu, S.; Liu, L. X.; Zhu, Z. Surface-Etched Halloysite Nanotubes in Mixed Matrix Membranes for Efficient Gas Separation. *Sep. Purif. Technol.* **2017,** *173*, 63-71.
(11) Ge, L.; Zhu, Z.; Li, F.; Liu, S.; Wang, L.; Tang, X.; Rudolph, V. Investigation of Gas Permeability in Carbon Nanotube (CNT)− Polymer Matrix Membranes via Modifying CNTs with Functional Groups/Metals and Controlling Modification Location. *J. Phys. Chem. C* **2011,** *115*, 6661-6670.
(12) Cong, H.; Zhang, J.; Radosz, M.; Shen, Y. Carbon Nanotube Composite Membranes of Brominated Poly (2, 6-diphenyl-1, 4-phenylene oxide) for Gas Separation. *J. Membr. Sci.* **2007,** *294*, 178-185.
(13) Sun, H.; Wang, T.; Xu, Y.; Gao, W.; Li, P.; Niu, Q. J. Fabrication of Polyimide and Functionalized Multi-Walled Carbon Nanotubes Mixed Matrix Membranes by in-Situ Polymerization for CO 2 Separation. *Sep. Purif. Technol.* **2017,** *177*, 327-336.
(14) Zhao, Y.; Jung, B. T.; Ansaloni, L.; Ho, W. W. Multiwalled Carbon Nanotube Mixed Matrix Membranes Containing Amines for High Pressure CO 2/H 2 Separation. *J. Membr. Sci.* **2014,** *459*, 233-243.
(15) Ansaloni, L.; Zhao, Y.; Jung, B. T.; Ramasubramanian, K.; Baschetti, M. G.; Ho, W. W. Facilitated Transport Mmembranes Containing Amino-Functionalized Multi-Walled Carbon Nanotubes for high-Pressure CO 2 Separations. *J. Membr. Sci.* **2015,** *490*, 18-28.